Association between Randall's plaque and calcifying nanoparticles

Neva Çiftçioğlu[a,d], Kaveh Vejdani[b], Olivia Lee[b], Grace Mathew[a,d], Katja M. Aho[c], E. Olavi Kajander[d], David S. McKay[e], Jeffrey A. Jones[e], Alan H. Feiveson[e], Marshall L. Stoller[b,*]

[a]*Nanobac Pharmaceuticals, Johnson Space Center, Houston, TX/USA,* [b]*Department of Urology, University of California at San Francisco, San Francisco, CA/USA,* [c]*University of Kuopio, Department of Biosciences/Biochemistry, Kuopio/Finland,* [d]*Nanobac Pharmaceuticals, Tampa, FL/USA,* [e]*National Aeronautics and Space Administration, Lyndon B. Johnson Space Center, Houston, TX/USA,* [f]*X*

* Corresponding author

Please add Dr. Stoller's contact info

Key words: Calcifying nanoparticles, nanobacteria, Randall's plaque, urinary stone

Word count of the text: 3522 (Limit 3000)
Word count of the abstract: 244 (Limit 250)
Take home message: A link was found between the presence of Randall's plaques and the detection of CNP, also referred to as nanobacteria. Further studies on this topic may lead us to new approaches on early diagnosis and novel medical therapies of kidney stone formation.

Abstract

Objectives: Randall initially described calcified subepithelial papillary plaques, which he hypothesized as nidi for kidney stone formation. The discovery of calcifying nanoparticles (CNP) in many calcifying processes of human tissues has raised another hypothesis about their possible involvement in urinary stone formation. This research is the first attempt to investigate the potential association of these two hypotheses.

Methods: We collected renal papilla and blood samples from 17 human patients who had undergone laparoscopic nephrectomy due to neoplasia. Immunohistochemical staining (IHS) was applied on the tissue samples using monoclonal antibody 8D10 (mAb) against CNP. Homogenized papillary tissues and serum samples were cultured for CNP. Scanning electron microscopy (SEM) and energy dispersive X-ray spectroscopy (EDS) analysis were performed on fixed papillary samples.

Results: Randall's plaques were visible on gross inspection in 11 out of 17 collected samples. IHS was positive for CNP antigen in 8 of these 11 visually positive samples, but in only 1 of the remaining 6 samples. SEM revealed spherical apatite formations in 14 samples, all of which had calcium and phosphate peaks detected by EDS analysis.

Conclusion. From this study, there was some evidence of a link between the presence of Randall's plaques and the detection of CNP, also referred to as nanobacteria. Although causality was not demonstrated, these results suggest that further studies with negative control samples should be made to explore the etiology of Randall's plaque formation, thus leading to a better understanding of the pathogenesis of stone formation.

1. Introduction

Seventy years ago, Randall performed a detailed examination of the papillae of more than 1,000 cadaveric renal units, and demonstrated that interstitial crystals located at, or adjacent to, the papillary tip were common in stone formers [1]. He found that these crystals were composed not of calcium oxalate (CaOx), the most common solid phase found in patients with nephrolithiasis, but of calcium phosphate (CaP) [2], and termed them as plaques. He believed that the CaP crystals precipitated in the papillary interstitium and subsequently eroded into the urinary space, serving as a nucleation surface for CaOx [2]. *In vitro*, CaP phases efficiently nucleate CaOx crystallization [3], so that one can easily conjecture that common CaOx stones begin on plaques. Recently, Matlaga et al have analyzed Randall's plaques and confirmed that they are formed of spherical, CaP particles [4]. Coe et al have also observed Randall's plaques with TEM and shown CaP deposits appearing as single spheres with a multilaminated internal morphology (Fig. 1 A and B). According to Merck Manual, all pathological calcifications contain snowball-like CaP spheres 200 nm in size [5]. However, the pathogenesis and identity of those spherical formations have remained elusive.

Structures similar to snowballs described by Merck Manual were discovered over a decade ago in blood and blood products [6]. These structures, known as nanobacteria, or CNP, were detected in numerous pathological calcification-related diseases [7-10]. The CNP are membrane-enclosed cell-like calcified vesicles [6], and they are morphologically and in mineral composition very similar to spherical bodies observed in Randall's plaques (Fig. 1). CNP contain no detectable genomic DNA or RNA, but yet appear capable of self propagation [11]. Due to lack of their genomic definition, CNP are controversial agents as prions were, and critics have proposed different hypotheses to

explain them as protein precipitates or crystal formation [12]. Although we know that CNP cause specific infection [13], and were detected in calcified tissue samples, general debate over their existence continues. Methods to detect CNP in biological samples include immuno-detection techniques using anti-CNP mAbs, specific culture techniques and electron microscopy [14]. With these methodologies, some important features of CNP and their triggering effect on nephrolithiasis have been suggested. These features include: **A)** CNP consist of tiny spheres (80-200nm) resembling "cells". They appear to precipitate apatite from their surrounding media forming apatite-protein complexes. Immunoelectronmicroscopy reveals protein antigens in close proximity to precipitated apatite, suggesting a novel form of protein-associated mineralization [15]. **B)** CNP mineralization starts as extremely small apatite crystals and forms on the exterior membrane of 80-200nm diameter CNP followed by a growing shell or an enclosing sphere of apatite which may reach a diameter of one to several micrometers [16]. **C)** 14% of healthy adults in Scandinavia have anti-CNP antibodies [17]. In comparison, a high fraction (75%) of patient groups with kidney diseases has CNP antigen in blood [18]. **D)** CNP form apatite units/shells *in vitro,* morphologically and chemically similar to those in the core of kidney stones, (Fig. 2) [19]. **E)** CNP are renotropic [20]. **F)** CNP cause kidney stone formation when injected into rats [21]. **G)** CNP have been detected in different types of kidney stones [19]. **H)** *In vitro*, destruction of the calcified apatite shell of CNP with EDTA-chelation reveals numerous 80 to 100nm diameter membranous cells [16] similar to those observed in Randall plaques by other research groups [4]. **I)** TEM study of renal plaques shows 1-5 μm apatite spheres laminated with mineral and organic molecules [4], similar to the structure of CNP (Fig.1) [6].

In this study, our aim was to investigate the association between the presence of CaP spheres found in Randall's plaques and detection of CNP. Such an association would be a basis for a formal hypothesis that can be discussed, and used to drive further studies in larger patient groups.

2. Materials and methods

2.1. Subjects

Renal papillae were dissected from 17 patients who had undergone laparoscopic nephrectomy due to neoplasia (Renal cell carcinoma, n=9; Transitional cell carcinoma, n=4; Other malignancies; n=4). Presence or absence of Randall's plaques was evaluated on gross inspection of immediately extracted and bivalved kidneys. Intact papillae were harvested well away from the tumor, and were prepared for the analyses with IHS, SEM, EDS and CNP culture. Blood was drawn in the fasting state from patients immediately before and after surgery. The serum was used for CNP culture, and enzyme-linked immunosorbent assay (ELISA) to detect CNP antigen and antibody. Bladder urine samples of patients were collected for routine bacterial culture. The study was approved by the UCSF Committee on Human Research and every patient was given detailed information regarding the procedures involved in this research and signed an informed consent prior to any manipulation.

2.2. Tissue preparation for analysis

Papillary specimens of 17 patients for IHS and SEM experiments were immediately immersed in 4% paraformaldehyde and refrigerated overnight. IHS samples were paraffin embedded and prepared for IHS as described earlier [22]. SEM samples were dehydrated and gold-coated as described previously [6]. The tissue samples for CNP cultures were immediately placed into 2ml of sterile phosphate buffered saline (PBS), pH 7.4, homogenized for 30-seconds, four times, with 30-second cooling intervals on ice using conventional, 5ml glass tissue-grinders. Homogenized tissue was centrifuged at 2500g for 15-minutes. The supernatant was separated and sterile-filtered through 0.22μm pore size, non-protein binding filters (Millipore) into sterile non-adhesive tubes and stored at -70°C until processed for culture as described below.

2.3. IHS analysis of papillary samples

Paraffin-embedded papillary samples were cut into 5μm sections, deparaffinized and rehydrated [22]. Each tissue section was demineralized in 250mM sodium citrate for 24 hours at +4°C, to retrieve apatite crystal-covered epitopes prior to IHS. After washing in water, endogenous peroxidase was blocked with 1% H_2O_2 in methanol for 30min. Slides were then rinsed in PBS before staining with a catalyzed signal amplification IHS (Dako, Carpinteria, CA, USA). Anti-CNP mAb, 8D10 (Nanobac Oy, Kuopio, Finland), was used as primary antibody which is recommended by the manufacturer for detection of CNP in formalin-fixed paraffin embedded tissue sections. All slides were counterstained with hematoxylin, and mounted with glycerol. Negative control sections went through the same staining process, except that the primary mAb step was omitted.

2.4. CNP cultures from serum and tissue samples

Patient serum samples, and homogenized tissue supernatant samples were cultured in Dulbecco's Modified Eagle's Medium (DMEM, Gibco Lab Inc., Grand Island, NY) under mammalian cell culture conditions (37°C, 5-10% CO_2, 90-95 % humidity) for 4 weeks. Patient sera were cultured at 10% final concentration, and tissue homogenates were cultured both with and without fetal bovine serum (FBS) supplementation (as a growth factor) which was previously tested for CNP and evaluated as CNP negative (Atlanta Biologicals, GA) as described earlier [14]. The pellets from the homogenized tissue were incubated with 30mM EDTA for 1-hour at room temperature for decalcification, and release of enclosed CNP from the apatite units, diluted 1:10 in DMEM, and cultured as described above. Each sample was filtered through 0.22μm pore-sized filters before culturing in order to eliminate potential conventional-bacterial contamination in a Biosafety level-2 facility. Cultures were checked for gross bacterial contamination by microscopy and macroscopic observation of turbidity and color change of the medium from the third day of incubation. Control culture plates, containing only culture media, were incubated in parallel with the test plates to determine whether spontaneous crystallization or precipitation can occur. Every week, the culture plates were inspected by phase contrast microscopy (Nikon Eclipse TE 2000-U) for CNP propagation. Positive identification of CNP involved typical slow propagation and optical properties, negative signal with Hoechst 33258 dye, and positive signal with indirect immunofluorescence staining (IIFS) [11]. Serum and tissue homogenate cultures for CNP were rated (-) = no growth in four weeks, (+) = growth in four weeks, (++) = growth in three weeks, (+++) = growth in two weeks, and (++++) = growth in one week of

incubation. All culture samples were harvested with 14000g centrifugation for 30 min at 4°C after 30 days of incubation. The pellets were spread on glass slides for IIFS, heat fixed and double-stained using CNP surface-antigen-specific mAb 8D10, followed by Alexa Fluor 488 goat-anti-mouse IgG secondary antibody [14]. In addition, Hoechst stain was used to detect conventional bacterial contamination. As a positive control for Hoechst, *E. coli* (nonpathogenic strain HB101) was used. Fluorescence photographs were taken using an Olympus BX60F5 microscope coupled to a Nikon digital camera DXM 1200F.

2.5. SEM and EDS microanalysis

Papillary samples 2-4 mm in block size were analyzed both for morphology and chemical composition using JEOL 6340 Field Emission SEM with attached IXRF EDS analyzer [6]. Each sample was divided into 4 mapping areas and each area was scanned for small, 100-500nm spherical forms, and calcium-rich or phosphate-rich particles. Cultured CNP and one oxalate kidney stone (provided by University of Kuopio Hospital/Finland) sample were prepared for SEM analysis using the same preparation technique for tissue samples. In EDS analyses, hydroxyapatite (Sigma, H-0252, St. Louis, MO) was used as a reference. SEM results were rated as (-) = no CNP observed; otherwise as the number of mapped areas in which CNP was seen (+ to ++++).

2.6. Biochemical Assays

The commercially available ELISA kits for detecting anti-CNP IgG and CNP-antigen; Nano-Sero IgG ELISA , and Nanocapture ELISA (Nanobac Oy, Finland) respectively

were used. All measurements were run in duplicates. Nano-Sero IgG ELISA is used to detect exposure to CNP. Antibody formation occurs after exposure to these agents [13]. Nanocapture ELISA measures quantitatively CNP antigen from a 50μl serum sample. The detection antibody recognizes CaP-binding protein-antigen on CNP in a special CaP complex conformation (ELISA kit inserts). There was not enough serum of subject #17 and therefore ELISA tests were not performed on this sample. For Nanocapture ELISA, a ratings were (-): < 3.5 units/ml; (+): 3.5-11.0 units/ml; (++): 11.0-50.0 units/ml; (+++): 50.0-150 units/ml; and (++++): > 150 units/ml. For Nano-sero ELISA, ratings were (-): < 0.1 units/ml; (+): 0.1 - 0.4 units/ml; (++): 0.4 - 0.5 units/ml; (+++): 0.5 - 0.7 units/ml; and (++++): > 0.7 units/ml.

2.7. Statistical analysis

Descriptive results of the various analytic techniques are displayed in terms of ratings in Table 2. Association between SEM findings and CNP growth ratings in tissue cultures was quantified in terms of contingency table analysis (Fisher Exact Test) with ratings collapsed to either 0 [rating = (-)] or 1 [rating = (+) – (++++)]. A similar analysis was made for possible association between SEM and ELISA_Ag concentration ratings.

3. Results

3.1. Subjects

Eleven male and 6 female patients were enrolled in our study, with a mean age of 65.5 and 78 years, respectively. Visually, Randall's plaques were observed on the papillae of

11 patients, with no sexual preponderance. No correlation was found between the observation of Randall's plaques and the patients' tumor types (Table 1). Urine cultures for conventional bacteria were negative in 12 patients, showed mild growth of genital flora in 3 patients and were positive for enterococcus species in 2 patients.

3.2. IHS

The results of papillae analyzed using IHS is summarized in Table 2. Nine out of 17 tissue samples stained positive for CNP antigen. Positive staining results, as a brown-colored precipitate at the antigen site, are shown in Fig.3 A, B and F. Negative controls that were stained with the same technique by omitting the mAb, did not show any non-specific signal (Fig 3 E). Eight papillary samples were negative with IHS (Figs.3 C and D).

3.3. CNP cultures of serum samples and tissue homogenates

All serum samples and 13 of 17 papillary tissue homogenates and tissue pellets contained propagating CNP at different growth rates (Table 2). The differences observed in the propagation rate may reflect existence of CNP in different concentrations. Three serum samples were already positive within three days of culture. All propagation-positive samples stained positive with IIFS using anti-CNP mAb, 8D10 (Fig. 4A), but stained negative with the Hoechst (Fig. 4B), indicating no bacterial contamination in cultures. The positive control for Hoechst dye, *E. coli,* was stained blue (Fig. 4C), but no nonspecific-signal was detected with 8D10 (Fig. 4D). SEM of cultured CNP showed

typical morphology of CNP (Fig. 5A), as described earlier [11]. In negative controls, no CNP growth, no mineralization or protein precipitation was observed.

3.4. SEM Analysis

Fourteen of 17 tissue samples contained CNP-like particles in various sizes (Fig. 5 B-D and Fig 6B). The tissue samples without visible, macroscopic plaques had fewer spherical apatite formations compared with samples with visible plaques (Fig. 7). The tissue cells with those apatite particles looked more deformed with fibrous formation (Figs. 5 C, D and 7F) whereas the negative tissue cells looked more intact (Figs. 6A and 7G). The apatite spheres produced an EDS pattern (Fig. 6C) identical to the CNP EDS patterns as observed in our earlier studies [6, 19].

In SEM analysis, oxalate kidney stone had spherical units in the core, similar to cultured CNP from renal plaques (Fig. 2) with identical EDS patterns.

3.5. ELISA

Out of 16 tested serum samples, 14 were positive for CNP-antigen, and 11 were positive for CNP-antibody. Nano-Sero IgG, and Nanocapture ELISA test results are summarized at Table 2.

3.6. Association between CNP and SEM detection of Randall's Plaques

Two-by-two contingency tables for SEM (detection of spherical apatite formations on renal papilla) versus tissue culture growth and SEM versus ELISA-Ag concentration ratings are shown in Tables 3 and 4, respectively. Note that 12 of 14 positive SEM

samples showed CNP growth, while 1 of 3 negative samples showed growth (Table 3, P = 0.121, Fisher's Exact Test). On the other hand the ELISA-Ag results were preponderantly positive regardless of the SEM results (Table 4, P = 0.650, Fisher's Exact Test).

4. Discussion

Plaques, defined as sites of interstitial crystal deposition at or near the papillary tip, are found in kidneys of CaOx-stone formers (100%) and often, but less frequently, in people who do not form CaOx stones (43%) [23]. The nucleus of these plaques are composed of CaP [24]. Despite extensive basic and clinical studies on Randall's plaques, the reason of CaP accumulation in the first place always remained elusive.

The discovery of CNP encapsulated in a CaP shell, and their subsequent detection in several human pathologic calcification processes, raised hopes for an explanation for Randall's plaques [16]. Soon after their discovery, the CNP were detected in human urinary stones [19, 25]. Inspired by these observations, we hypothesized that CNP might actually be the initiating agents in the formation of Randall's plaques and subsequently the renal stones. CNP resemble the snowballs from pathological calcifications, described by Merck Manual "cell" size (~0.1-0.5μm). In addition, they cause rapid *in situ* precipitation of CaP from blood and other body fluids under conditions not normally conducive to such precipitation [6]. CNP are renotropic, as reported from rabbit experiments using injected radiolabelled-CNP and are eliminated from the circulation through urinary excretion [20]. It was also shown that translumbar, percutaneous

intrarenal injection of CNP into rats resulted in kidney stone formation [21]. Whether CNP themselves serve as the nucleus for crystal formation, or they are simply able to lower the activation energy barrier and thus allow precipitation and growth of crystals under much lower supersaturation conditions is yet to be determined.

In this study, we investigated the presence of CNP in the Randall's plaques of non stone-forming human patients. For apparent reasons, kidneys could not be obtained from healthy subjects to serve as negative controls. Similarly, kidneys from renal stone patients are normally not removed, unless complicated by severe hydronephrosis or superimposed pyelonephritis / pyonephrosis. All subjects in our study had their kidneys removed due to a renal mass.

We observed Randall's plaques in 65% of the extracted kidneys, and searched for CNP in the renal papillae through IHS, SEM and culture techniques. 72% of plaque-positive tissues were positive for CNP antigen in IHS. IHS was negative in 83% of plaque-negative tissues, indicating a statistically significant association ($p=0.043$). Negative IHS result in a plaque-positive sample could be due to the fact that a section plane might not cut through the plaque or the plaque is lost during the processing because it is very hard tissue, and difficult to cut. On the other hand, visually plaque-negative sample might stain positive if CNP antigen is actually present in the tissue but macroscopically invisible.

SEM provides additional information regarding the presence or absence of CNP through the distinctive morphology of these particles (Fig. 5). SEM of papillae revealed CNP-like spheres in the majority of the samples, irrespective of the presence of visible Randall's plaques. As with IHS, CNP morphology might not be observed in a plaque-

positive tissue if the plaque does not pass through the tissue surface inspected under SEM, or be detected in a visually plaque-negative sample if plaques are too small.

In our earlier TEM analysis of CNP shells we defined their morphology as "tree-age-ring-like" formations of crystal and organic matter [26], a description which is almost identical to observations in Randall's plaques (Fig. 1) by others [24]. We also have observed apatite spherical formations in the core of kidney stones independent of their overall chemical composition (Fig. 2), and cultured CNP from those stones [19].

In EDS analysis, the CNP-like spheres on paplillae produced calcium and phosphate peaks identical to that of the CNP in previous reports. No calcium-phosphate peaks were detected in tissues without CNP-like spheres.

To see if these apatite spheres are actually capable of propagating, a typical property of CNP of potential pathogenic importance in stone growth or formation, we cultured the papillary tissue extracts obtained from our patients. All but one sample grew CNP within 4 weeks (Table 2), as identified by IFS of harvested culture pellets with the CNP-specific mAb. We cultured patient serum samples obtained before and after surgical manipulation, all of which turned positive within 4 weeks (Table 2). ELISA tests measuring CNP antigen (15/16) and antibody (11/16) in patient blood are also strongly correlated with culture results.

To a great extent, our studies accord with and confirm much of Randall's pioneering work. The plaque is interstitial and composed of apatite. What we add, here, is that many of the apatite formations are culturable and stainable with CNP-specific mAb. Therefore one conclusion could be that Randall's plaques contain CNP. Where do these CNP come from? Stoller et al suggested vascular origin of Randall's plaques [27]. We have detected

CNPs in blood [6]. The described elimination route via kidneys into urine may be a way for CNP to form an infectious foci or agglomeration in the kidneys. Infectious foci may form the Randall's plaque [26]. Interestingly, CNP have been also detected in calcifications of atherosclerosis [8]. In both these cases, as pathological calcification in general, CaP particles 200 nm in size have been observed. Thus, CNPs could be the long looked for 200 nm CaP snowballs present in pathological calcification.

The finding of CNP in Randall's plaque needs to be confirmed with a prospective research design including a larger patient population and negative controls. We have developed diagnostic tools for this unique agent, and also found that CNP are susceptible to certain antibiotics [28]. If supported by further work, this hypothesis may lead to treatment designed to disable the CNP, prevent or control the precipitation of apatite, and treat the formation of kidney stones as a consequence of an infection.

5. Conclusion

With this small and retrospective study, we found some evidence of a link between the presence of Randall's plaques and the detection of CNP, also referred to as nanobacteria. These results suggest that further studies with negative control samples should be made to explore the etiology of Randall's plaque formation, thus leading to a better understanding of the pathogenesis of urolithiasis.

References

[1]. Randall A. The origin and growth of renal calculi. Ann Surg 1937 ; 105:1009-27.

[2]. Randall A. Papillary pathology as precursor of primary renal calculus. J Urol 1940 ; 44:580-89.

[3]. Mandel GS, Mandel NS. Crystal-crystal interactions, In : Coe FL, Favus MJ, Pak CYC, Parks JH, Preminger GM, editors. Kidney stones: medical and surgical management. Lippincott-Raven Publishers, Philadelphia, Pennsylvania, USA 1996, p. 115–28.

[4]. Matlaga BR, Coe FL, Evan AP, Lingeman JE. The role of Randall's plaques in the pathogenesis of calcium stones. J Urol. 2007; 177:31-38.

[5]. Merck Manual of Diagnosis and Therapy. November 2005. Section 5, Chapter 55. http://www.merck.com/mmpe/sec04/ch035/ch035d.html?qt=BCP&alt=sh

[6]. Kajander EO, Çiftçioglu N. Nanobacteria: An alternative mechanism for pathogenic intra- and extracellular calcification and stone formation. Proc. Natl. Acad. Sci. USA 1998 ; 95:8274-79.

[7]. Shoskes DA, Thomas KD, Gomez E. Anti-nanobacterial therapy for men with chronic prostatitis/chronic pelvic pain syndrome and prostatic stones: preliminary experience. J Urol 2005 ; 173:474-77.

[8]. Miller VM, Rodgers G, Charlesworth JA, et al. Evidence of nanobacterial-like structures in calcified human arteries and cardiac valves. Am J Physiol Heart Circ Physiol 2004 ; 287:1115-124.

[9]. Hudelist G, Singer CF, Kubista E, et al. Presence of nanobacteria in psammoma bodies of ovarian cancer: evidence for pathogenetic role in intratumoral biomineralization. Histopathology 2004 ; 45:633-37.

[10]. Wen Y, Li YG, Yang ZL, et al. Detection of nanobacteria in serum, bile and gallbladder mucosa of patients with cholecystolithiasis. Chin Med J 2005 ; 118:421-24.

[11]. Çiftçioglu N, McKay DS, Mathew G, Kajander EO. Nanobacteria: fact or fiction? Characteristics, detection, and medical importance of novel self-replicating, calcifying nanoparticles. Journal of Investigative Medicine 2006 ; 54:385-94.

[12]. Cisar JO, Xu DQ, Thompson J, Swaim W, Hu L, Kopecko DJ. An alternative interpretation of nanobacteria-induced biomineralization. Proc Natl Acad Sci USA 2000; 21:11511-5.

[13]. Çiftçioglu N, Aho KM, McKay DS, Kajander EO. Are apatite nanoparticles safe? Lancet 2007; 9579:2078.

[14]. Miller-Hjelle MA, Hjelle JT, Çiftçioğlu N, Kajander EO. Nanobacteria: Methods for growth and identification of this recently discovered calciferous agent. In : Wayne P. Olson, editor. Rapid Analytical Microbiology. The Chemistry and

Physics of Microbial Identification. PDA Bethesda, MD, USA, Davis Horwood International Publishing, Ltd, Godalming. Surrey, UK, 2003. p. 297-312.

[15]. Vali H, McKee MD, Çiftçioğlu N, Sears SK, Plows FL, Chevet E, Ghiasi P, Plavsic M, Kajander EO, Zare RN. Nanoforms: A new type of protein-associated Mineralization. Geoch Cosmoch Acta 2001; 65: 63-74.

[16]. Kumar V, Farell G, Yu S, Harrington S, Fitzpatrick L, Rzewuska E, Miller VM, Lieske JC. Cell biology of pathologic renal calcification: contribution of crystal transcytosis, cell-mediated calcification, and nanoparticles. J Investig Med 2006; 54:412-24.

[17]. Holmberg M. Prevalence of Human Anti-Nanobacteria Antibodies Suggest Possible Zoonosis. 1st International Minisymposium on Nanobacteria, Kuopio, Finland, 2001, (http://www.nanobac.fi/nbminisymp080301/page10.html).

[18]. Hjelle JT, Miller-Hjelle MA, Poxton IR, Kajander EO, Çiftçioglu N, Jones ML, Caughey RC, Brown R, Millikin PD, Darras FS. Endotoxin and nanobacteria in polycystic kidney disease. Kid Int 2000 ; 57: 2360-74.

[19]. Çiftçioglu N, Björklund M, Willman K, Kuorikoski K, Bergström K, Kajander EO. Nanobacteria: an infectious cause for kidney stone formation. Kid Int 1999; 56:1893-98.

[20]. Åkerman KK, Kuikka JT, Çiftçioglu N, Parkkinen J, Bergström KA, Kuronen I, Kajander EO. Radiolabeling and in vivo distribution of nanobacteria in rabbit. In : Richard B. Hoover, editor. Instruments, Methods, and Missions for Astrobiology, The International Society for Optical Engineering, Proceedings of SPIE, 1997. 3111: 436-42.

[21]. García Cuerpo E, Kajander EO, Çiftçioğlu N, Castellano FL, Correa C, Gonzales J, Mampaso F, Liano F, De Gabiola ED, Berrilero YAE. Nanobacteria ; Un modelo de neo-litogenesis experimental. Arch. Esp. de Urol 2000 ; 53: 291-303.

[22]. Scheffer GL, Hu X, Pijnenborg AC, Wijnholds J, Bergen AA, Scheper RJ. MRP6 (ABCC6) detection in normal human tissues and tumors. Lab Invest 2002 ; 82:515-18.

[23]. Low, RK, Stoller ML. Endoscopic mapping of renal papillae for Randall's plaques in patients with urinary stone disease. J Urol 1997 ; 158:2062-64.

[24]. Coe FL, Evan A, Worcester E. Kidney stone disease. J Clin Invest 2005 ; 115: 2598-2608.

[25]. Shiekh FA, Khullar M, Singh SK. Lithogenesis: induction of renal calcifications by nanobacteria. Urol Res 2006; 34: 53-7.

[26]. Kajander EO, Çiftçioglu N, Aho K, Garcia-Cuerpo E. Characteristics of nanobacteria and their possible role in stone formation. Urol Res 2003; 31:47-54.

[27]. Stoller ML, Low RK, Shami GS, McCormick VD, Kerschmann RL. High resolution radiography of cadaveric kidneys: unraveling the mystery of Randall's plaque formation. J Urol 1996;156:1263-6.

[28]. Çiftçioğlu N, Miller-Hjelle MA, Hjelle JT, Kajander EO. Inhibition of nanobacteria by antimicrobial drugs as measured by modified microdilution method. Antimicrob Agents Chemother 2002; 46:2077-86.

Titles and legends for figures

Figure 1. Morphological similarities of published TEM images of spherical, apatite

containing formations in renal papilla (A and B), and CNP (C and D). Magnifications: A,

20,000X; B 30,000X; C and D, bars 200nm.

Reprinted from; A: Coe FL, Evan A, Worcester E. Kidney stone disease. *J Clin Invest*.

115:2598-2608, 2005 [24] with permission from American Urological Association. B:

Matlaga BR, Coe FL, Evan AP, Lingeman JE. The role of Randall's plaques in the

pathogenesis of calcium stones. *J Urol*. 177:31-38, 2007 [4] with permission from

American Urological Association. C: Kajander EO, Ciftcioglu N. Nanobacteria: an

alternative mechanism for pathogenic intra- and extracellular calcification and stone

formation. *Proc Natl Acad Sci U S A*. 95:8274-8279, 1998 [6] with permission from

copyright 1998 National Academy of Sciences USA. D: Kajander EO, Ciftcioglu N, Aho

K, Garcia-Cuerpo E. Characteristics of nanobacteria and their possible role in stone

formation. *Urol Res.* 31:47-54, 2003 [26] with kind permission from Springer Science

and Business Media.

Figure 2. SEM images of apatite spheres in various sizes in the core of an oxalate kidney

stone (A), apatite formations in the CNP culture (B). Bars= A; 1μm, B; 10μm.

Figure 3. Immunohistochemical (IHS) staining of paraffin embedded renal tissue by

using anti-CNP monoclonal antibody. Brown color shown by black arrows indicates

positive signal (existence of CNP antigen) in the tissue. The images shown at A (100X)

and B (200X) are from renal plaque positive, IHS-positive tissue. C (100X) and D (400X) are from IHS-negative tissue, E and F (200X) are consecutive sections from a positive tissue. E is stained by omitting the monoclonal antibody, showing no positive signal whereas in F positively stained in one of the collecting ducts.

Figure 4. Light microscopic images of double staining results of patient samples cultured under CNP culture conditions. (A) IIFS positive cultured patient sample recognizing the CNP specific monoclonal antibody when imaged with the green bandpass emission filter, (B) Negative results of Hoechst die the same sample (A) imaged with the blue bandpass emission filter. (C) IIFS negative bacterial control (nonpathogenic *E. coli* strain HB101) not recognizing the CNP specific monoclonal antibody with green bandpass emission filter. (D) Positive results of Hoechst die the same sample (C) imaged with the blue bandpass emission filter.

Figure 5. SEM images of (A): cultured CNP from a serum sample, (B, C, and D): CaP spheres detected on renal papilla (Randall's plaque). Bars; 2μm.

Figure 6. SEM analysis of renal papilla and EDS analysis. A, Renall cells with no plaques. B, renal cells with plaque formations showing bumpy surface. White arrows show the spherical apatite formations on cells. C, EDS analysis of the one representative apatite sphere on the cells shown in B.

Figure 7. Images from Randall's plaques. (A) Tiny calcifications at the tip of the renal papilla. (B) Relatively large calcified plaques. (C) A cross section through the renal papilla, showing sub-epithelial calcifications running deep into the renal medulla. A closer images of renal papilla tissue with (D) and without eye-visible plaque formations (E). (F) and (G) are SEM images of the tissues shown at (D) and (E) respectively. Black arrows show streaks of plaques on the tissue, white small arrows show the apatite spheres on the tissue. Bars: F and G are 10μm.

FIGURES

Figure 1.

Detected
spheres in
Randall's
plaques

Calcifying
Nanoparticles
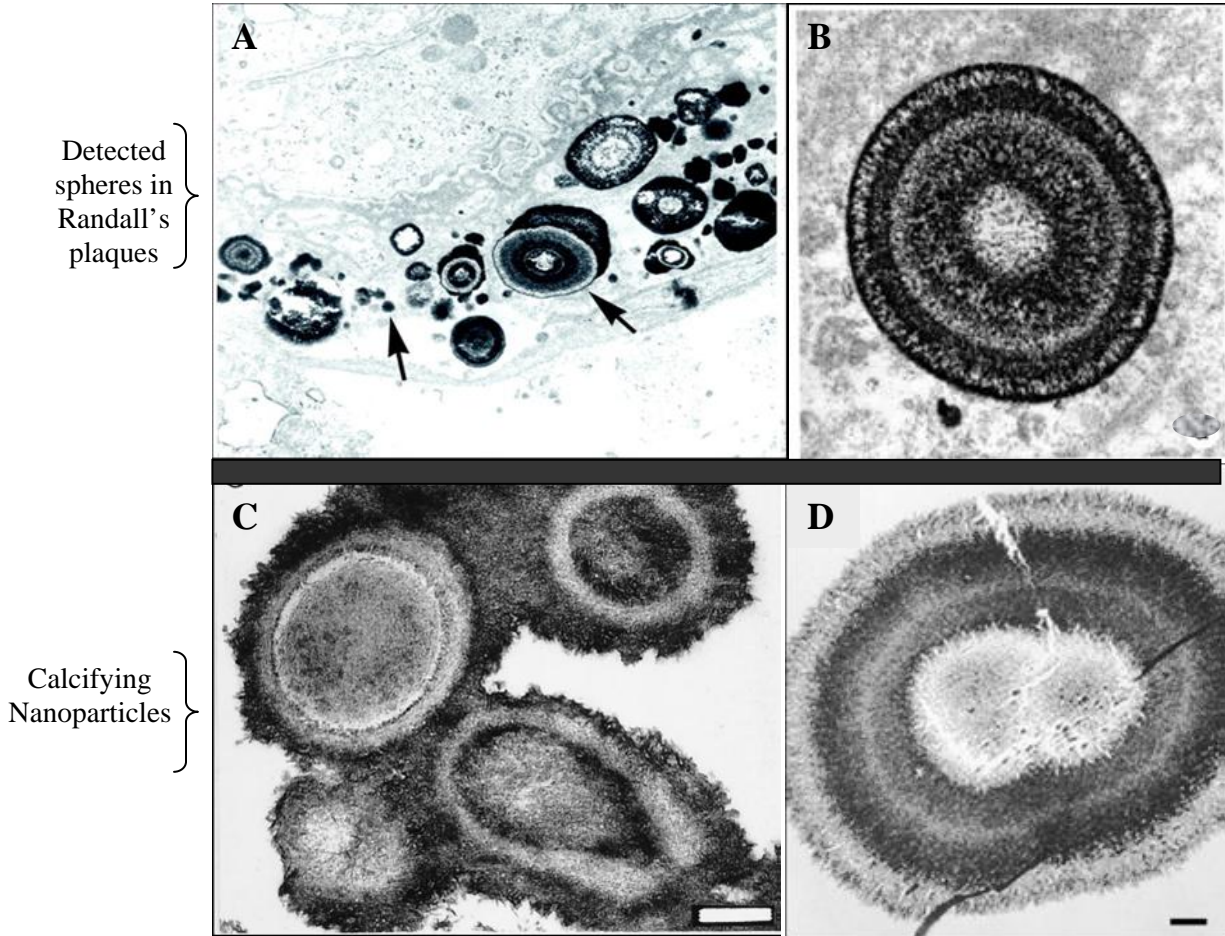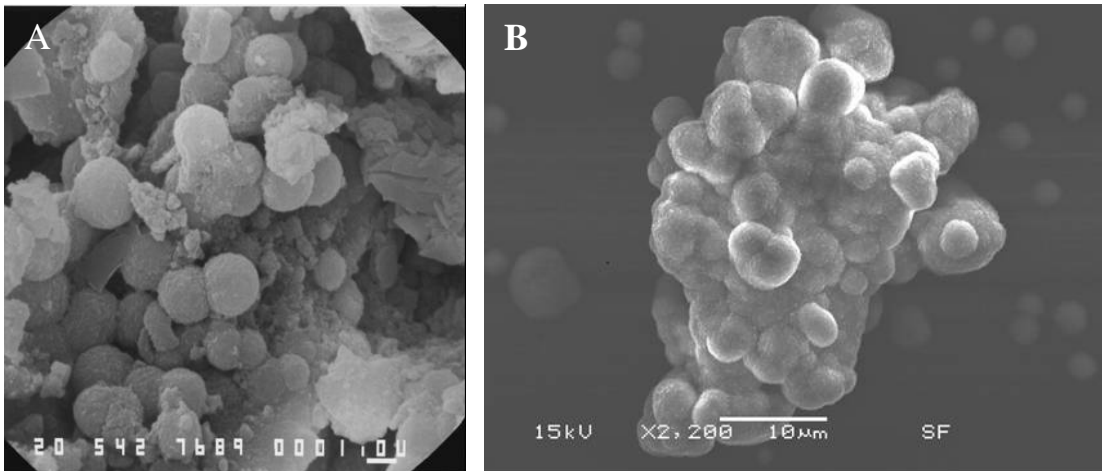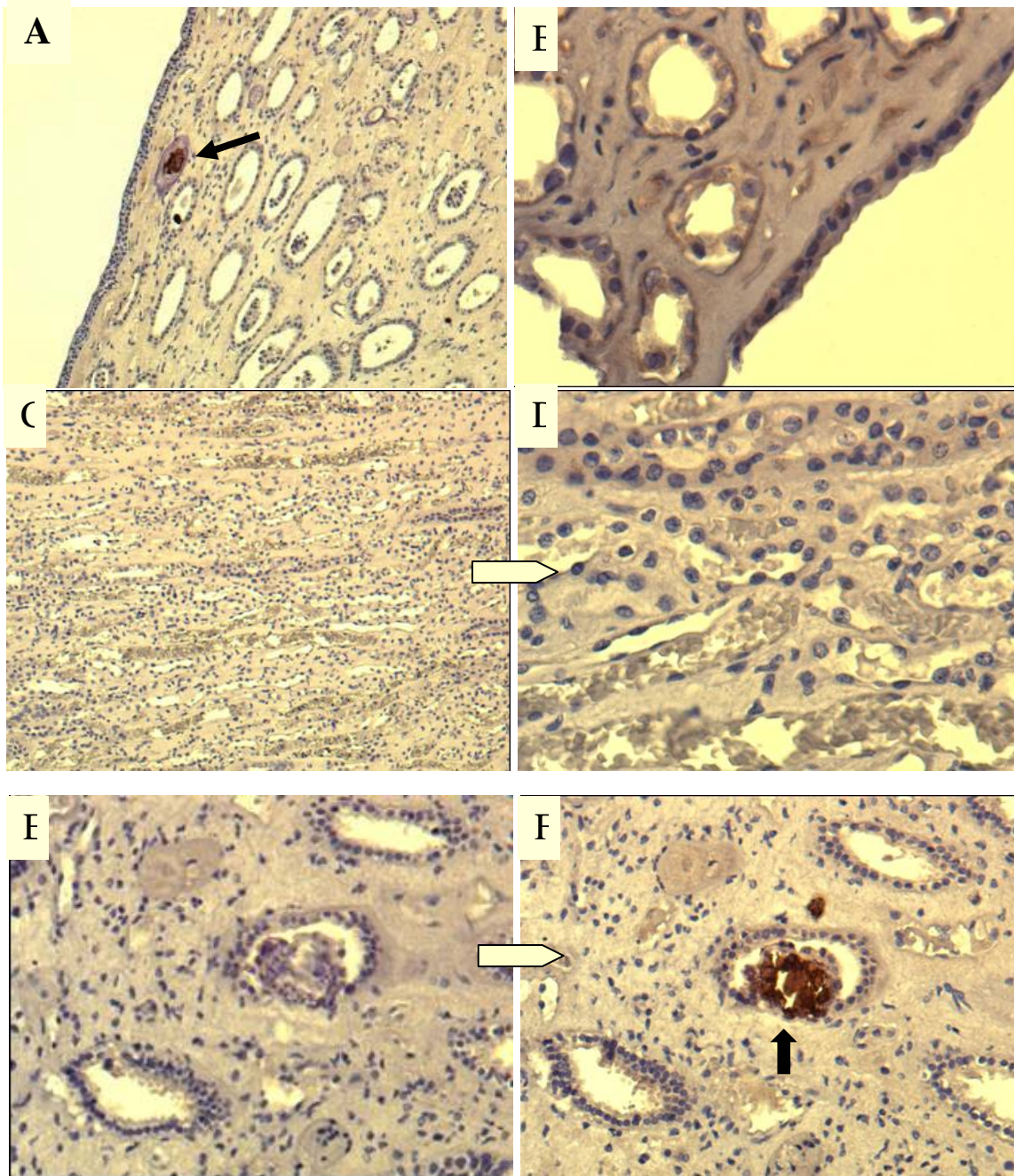
Figure 2.

Figure 3.

Figure 4.
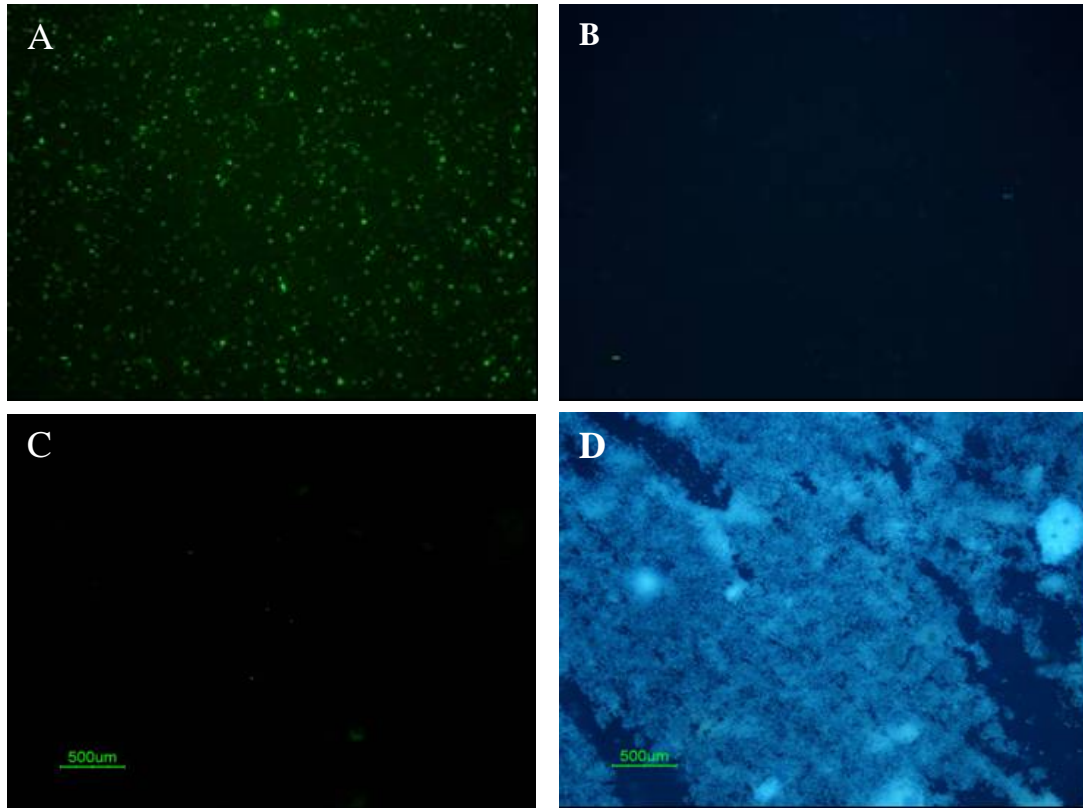
Figure 5.
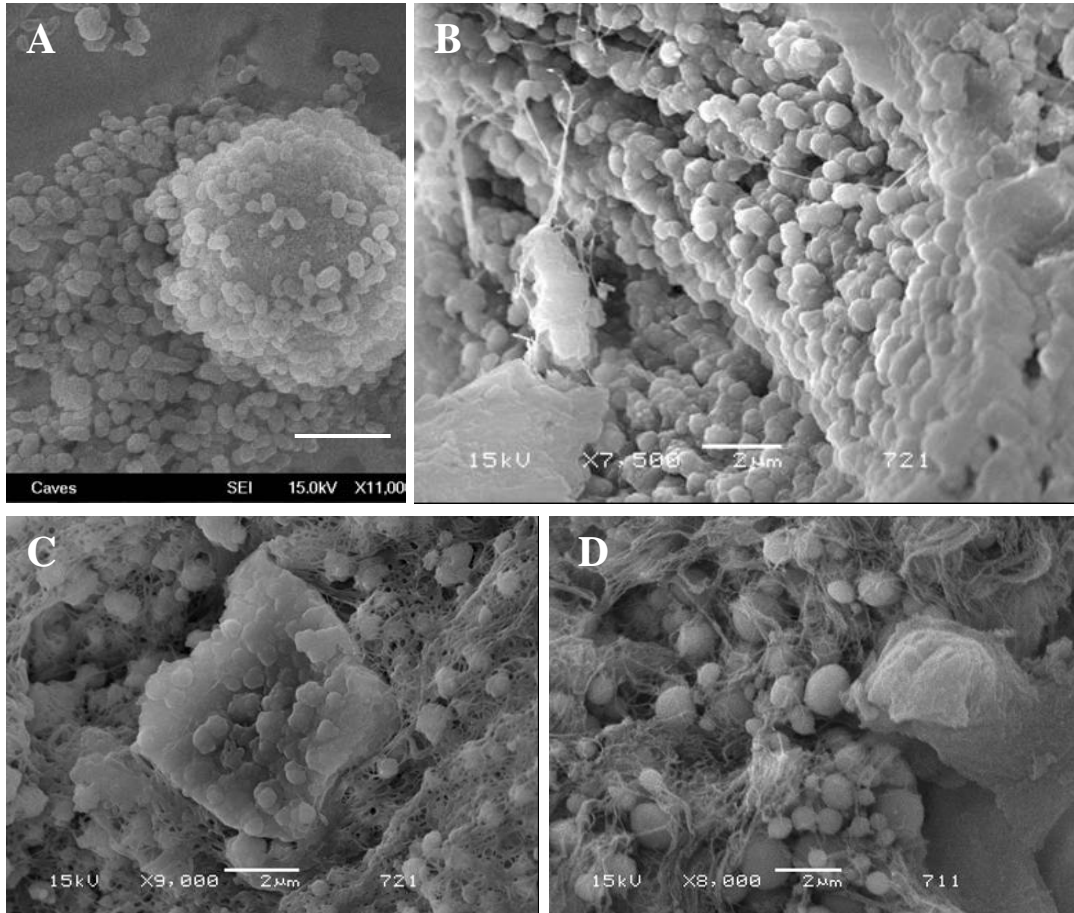
Figure 6.
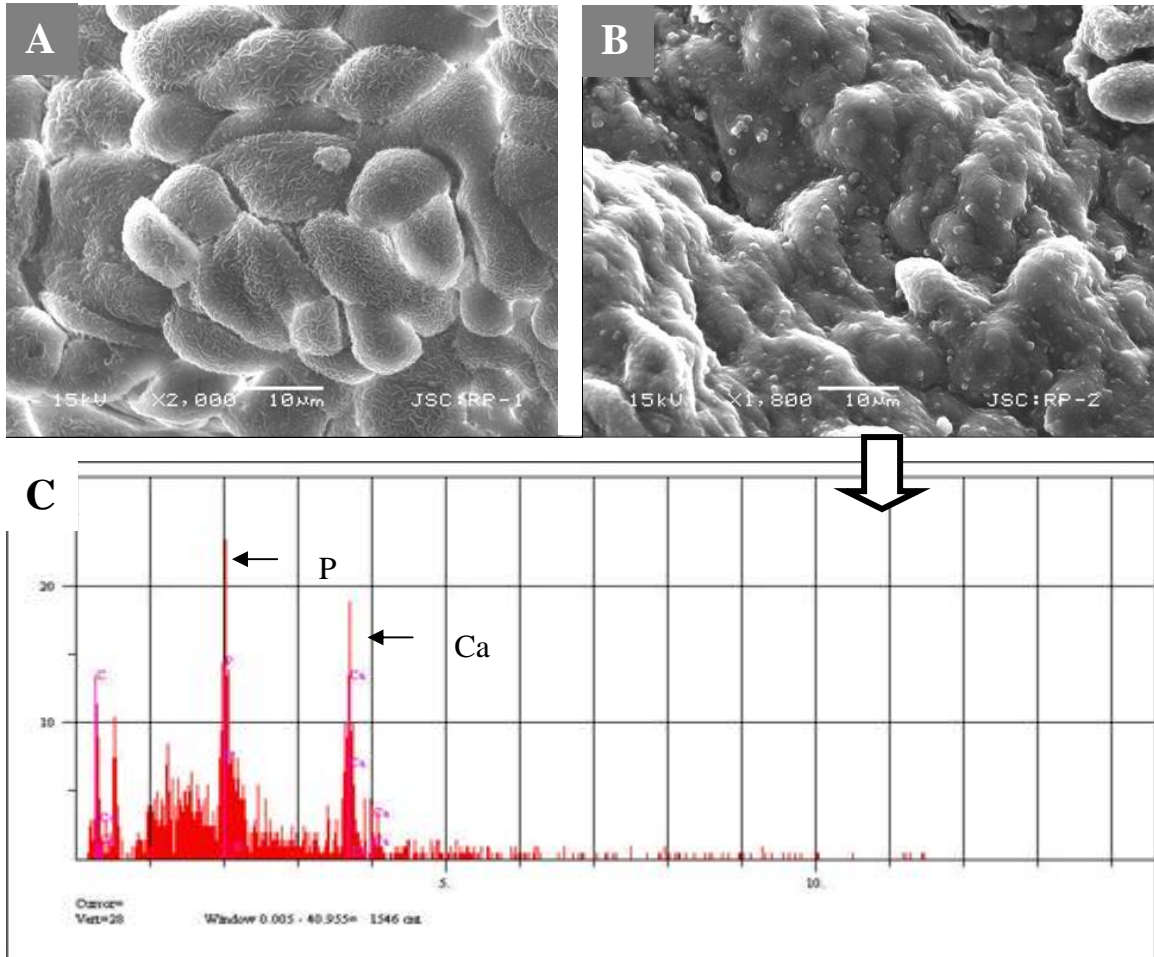
Figure 7.
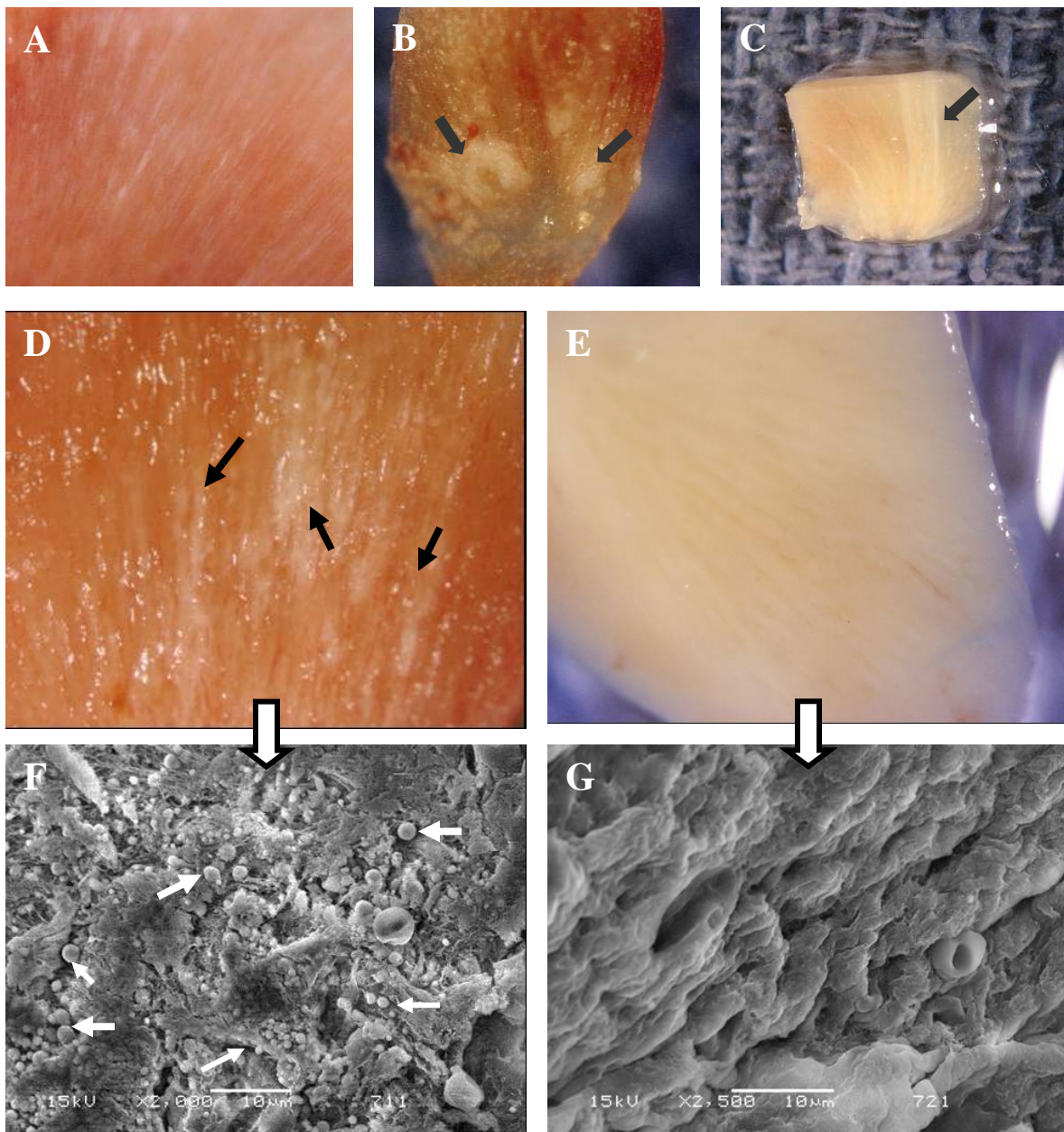
Table 1. Association between the observation of Randall's plaques and the patients'

tumor types.

Diagnosis	RP +	RP -	p-value (chi-square test of diagnosis versus RP)
RCC	4	5	0.18
TCC	3	1	0.92
Other *	4	0	0.28

RCC: Renal cell carcinoma
TCC: Transitional cell carcinoma
* Including oncocytoma and medullary fibroma

Table 2. Observation of Randall's plaques on gross inspection, and the detection of CNP by various methods**.**

Sample No	Tissue Analysis					Blood Analysis		
	Randall's plaques	IHC	SEM	EDS	Tissue homogenate culture for CNP	Serum culture for CNP	ELISA Ag	ELISA Ab
1	-	-	-	-	-	+++	+	-
2	+	+	+++	+	-	+++	+	+
3	+	+	+++	+	++	++	+++	-
4	+	-	+++	+	+	+	+++	+
5	+	+	+	+	++	+++	++	-
6	+	+	+++	+	++	++++	-	-
7	-	-	+++	+	++	+++	+	-
8	+	+	++++	+	+	++++	++++	+
9	-	-	++++	+	+	++++	++++	+
10	-	+	+++	+	++	++	++	+
11	-	-	++	+	+	+	-	+
12	+	+	-	-	-	+	++++	+
13	-	-	+++	+	-	+	++	+
14	+	+	+	+	+	+	++	+
15	+	+	-	-	+	+	++++	+++
16	+	-	++	+	+	+	++	+
17	+	-	+	+	+++	+++	ND	ND
Positive	11	9	14	14	13	17	14	11

CNP: calcifyin nano particles, IHC: Immunohistochemistry, SEM: scanning electron microscopy; EDS; energy dispersive X-ray spectroscopy; ND: Not done.
The serum and tissue homogenate cultures for CNP have a rating of ++++: growth in one week, +++: growth in two weeks, ++: growth in three weeks, +: growth in four weeks, -: no growth in four weeks of incubation. SEM is rated as 0 if no CNP is observed, 1 if CNP are seen in one of the four mapped areas, 2 if CNP are seen two of the four mapped area, 3 if CNP are seen three of the four mapped area, and 4 if CNP are seen in every scanned area at 1500X magnification. ELISA results are rated according to the ELISA kit manufacturer's "1 unit" definition.

Table 3. Fisher's exact analysis of SEM/EDS test results versus CNP propagation from the papillary tissue results.

SEM/EDS	CNP propagation from the tissue homogenate		Total
	0	**1**	
0	2	1	3
1	2	12	14
Total	4	13	17

Fisher's exact = 0.121
1-sided Fisher's exact = 0.121

Table 4. Fisher's exact analysis of SEM/EDS test results versus ELISA-Ag test results.

SEM/EDS	ELISA-Ag results		Total
	0	**1**	
0	0	3	3
1	2	11	13
Total	2	14	16

Fisher's exact = 1.000
1-sided Fisher's exact = 0.650